

## **FINITE ELEMENT CALCULATION OF SWEDISH RESCUE CENTRES (RC 90) AND SHELTERS**

L Laine, ANKER – ZEMER Engineering A/S, Norway  
O Hedman, SWEDISH RESCUE SERVICE AGENCY, Sweden

### **Abstract**

RC 90 is designed to resist conventional weapons. A procedure for the simulation of air blast and ground shock on RC 90 is to be developed. The simulations accounting for fluid / structure interaction give a qualitative prediction of the response of RC 90 to a distant detonation.

Keywords: air blast, ground shock, fluid / structure interaction, numerical simulations, high explosives, concrete, soil, building

### **1. Introduction**

In Sweden Rescue Centres ("RC 90") are built and planned for the accommodation of the civil defence command during preparedness and war. The RC 90 is always combined with fire-fighting services. This gives the RC 90 a meaningful use in peace. The Rescue Centres are constructed as one-, or two storey buildings. Often, one floor is below ground surface. The framework is made of reinforced concrete, where the walls are made 400 to 800 millimetres thick. The RC 90 is not made 'hit proof' for cost reasons. RC 90 is designed to resist conventional weapon loads that detonate at a distance from the structure.

The protection of installations and personnel against vibrations and shock accelerations is important in order to uphold the commanding function after this type of loads. Deformations and crushing that take place in the protective structure may occur as long as the building is functionally intact.

Air blast, debris and ground shocks are the typical weapon loads that are generated. These loads introduce shock waves into the protective structure of a RC 90. Such loads can be calculated and taken into account with explicit finite element codes, like LS-DYNA [1]-[3] utilised for the simulations reported here. To calculate the weapon loads on the structure, fluid / structure interaction is accounted for, using an ALE formulation for a mix of three materials: Explosive, air, and soil. The concrete structure of a typical RC 90 is modelled with solid Lagrange elements, with smeared solid layers of reinforcement.

The potential threat corresponds to the general purpose bomb of type MK-82, an equivalent charge weight of TNT is used, [4]. The stand off distance to RC 90 is set to 5 [m], assuming a partially buried weapon. The simulations account for the soil, saturated sandy clay with small amounts of air voids (less than 1 percent), its seismic sound speed being 1500 metres per second and its density 1900 kilograms per cubic meter. The calculated ground shock velocities and pressures are compared with [4].

This paper focuses on the use of numerical calculations to predict the weapon loads, air blast and ground shock, and the response of the protective structure of the RC 90.

## 2. Boundaries, processors (Lagrangian and ALE) and coupling

Two symmetry planes are used in the finite element model, they intersect in the centre of gravity of the charge. Non reflecting boundary surface is used for the fluid to limit the extension of the fluid when the soil is considered. Vertical boundary constraints are applied to the nodes at the bottom surface of the ground floor. A frame of nodes (with thickness 0.5 [m] ) on the far side of the structure is given ground constraints.

The ALE-fluid is accomplished with an split operation technique, at each calculation cycle the calculations are performed with a Lagrangian phase followed by a rezoning and advection phase. In the advection phase, conservative variables, mass, momentum and energy are transported, using first order advection algorithm (donor cell + half index shift). The number of Lagrangian cycles between advection phases is set to one. This technique is used to accomplish a fixed mesh EULER. A multi-material algorithm (SLIC) available in LS-DYNA, allowing two and three materials within a single element. A simple line interface calculation is used for the advection of material between mixture elements, [1]-[3].

Fluid / structure interaction is used to pass information from the ALE-fluid to Lagrangian structure. The fluid mesh has to overlap the Lagrangian mesh for interaction to occur. All nodes of the ALE elements that contain one lagrangian point are coupled, [3].

## 3. Geometric model

A parametric geometric model of a typical Rescue Centre type RC 90 and soil, explosive, and air combined in a "fluid" is generated with ANSYS/LS-DYNA, [2]. The position and size of the charge, the wall thickness, and the size of the building, as well as the mesh can easily be changed by parameter variation. The dimensions used are: Fluid:  $x_{\text{fluid}} = 5.0$  [m],  $y_{\text{fluid}} = 6$  [m], and  $z_{\text{fluid}} = 6$  [m], RC 90:  $x_{\text{structure}} = 12.0$  [m],  $y_{\text{structure}} = 6.0$  [m],  $z_{\text{structure}} = 6.0$  [m], outer wall and floor thickness = 0.5 [m], middle floor thickness = 0.25 [m], and inner wall thickness = 0.2 [m]. The covering concrete layer is 0.04 [m] thick. The smeared reinforcement layers are 0.04 [m] thick. The layout of the model is shown at figure 1.

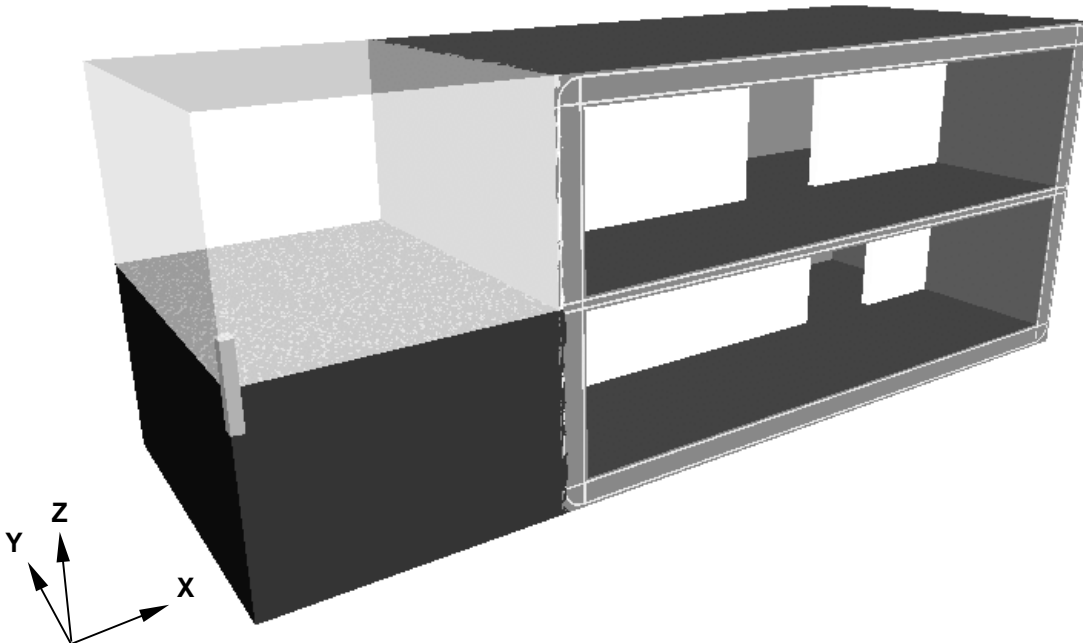


Fig. 1 Geometric model, the charge is half buried in the soil, the inner walls is inline with the x-z plane at  $y=3.0$  [m].

The total number of elements in the fluid is approximately 220 000. The protective structure of RC 90 is modelled by of approximately 70000 Lagrange elements. Eight node elements with one integration point are used in the protective structure. In figure 2-3 mesh details of the corner and the middle floor connection of the protective structure are shown.

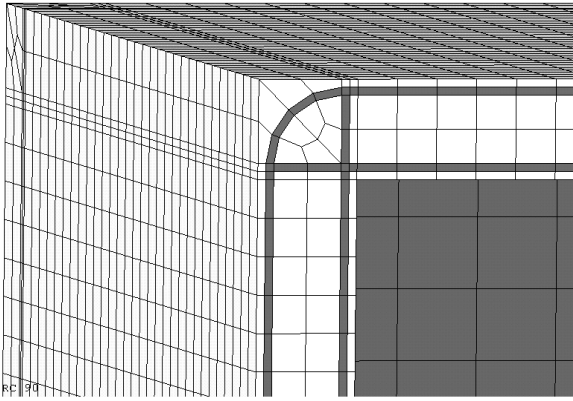


Fig. 2 Detail of how the outer corners are meshed.

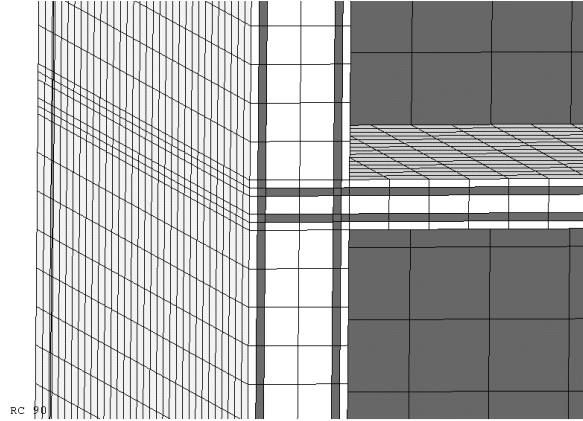


Fig. 3 Detail of mesh at the connection of outer walls and middle floor.

#### 4. Material models and equation of state

##### 4.1 Air

The air is modelled with the Null material model. This model allows equation of state (“EOS”) to be considered without computing the deviatoric stresses. The Linear polynomial EOS is used, this EOS is used to represent a gas following the gamma law. A modified gamma law EOS is used:

$$p = (\gamma - 1) \cdot \frac{\rho}{\rho_0} \cdot E + C_0 \quad (1)$$

Initial properties are:  $\rho_0=1.3$  [kg/m<sup>3</sup>],  $\gamma=1.4$  [-],  $E=250$  [kPa] and the constant  $C_0=-100$  [kPa]. The constant,  $C_0$  is added to avoid complications in problems with multi-materials where initial small pressures would generate unwanted velocities, this gives a starting pressure near zero, [6].

##### 4.2 Explosive

The TNT, having an initial density of 1630 [kg/m<sup>3</sup>], detonation velocity of 6930 [m/s], and the Chapman-Jouget pressure 21.0 [GPa], is modelled using the material model High explosive burn with the Jones-Wilkins-Lee (“JWL”) EOS. Material parameters for different explosives can be found in, [7]. The JWL EOS is:

$$p = A \cdot \left(1 - \frac{\omega}{R_1 \cdot V}\right) e^{-R_1 \cdot V} + B \cdot \left(1 - \frac{\omega}{R_2 \cdot V}\right) e^{-R_2 \cdot V} + \frac{\omega \cdot E}{V} \quad (2)$$

Input parameters used for the TNT are;  $A=373.8$  [GPa],  $B=3.747$  [GPa],  $R_1=4.15$  [-],  $R_2=0.9$  [-],  $\omega=0.35$  [-],  $E_0=6.0 \cdot 10^9$  [J/m<sup>3</sup>] and  $V_0=1.0$  [-].

##### 4.3 Soil

The soil, saturated sandy clay, is modelled with the Elastic plastic hydro material model. The Tensor pore collapse EOS is used. For saturated clays the water content has profound influence on ground shock propagation. When the saturation approaches one hundred percent, peak stresses and accelerations similar to shock wave propagation in free water have been observed, [4]. In saturated clays and saturated sandy clays the shear strength is small, thus the influence of the shear waves is small. The compressive shock wave is the dominant effect in loose soil materials, [8].

The assumed material properties are: initial density is 1900 [kg/m<sup>3</sup>], the shear modulus is 1.01 [GPa], the yield stress 400 [kPa], plastic hardening modulus 0.1 [kPa]. The pressure cut off was set to a small negative value. Literature on soil can be found in [9] - [11].

The EOS used for saturated sandy clay is shown in figure 4. The virgin loading curve is similar to water and the completely crushed curve is assumed to intersect at  $\mu_2=0.16$  [-] and  $p_2=676.0$  [MPa]. The elastic limit used is,  $\mu_1=1 \cdot 10^{-4}$  [-].

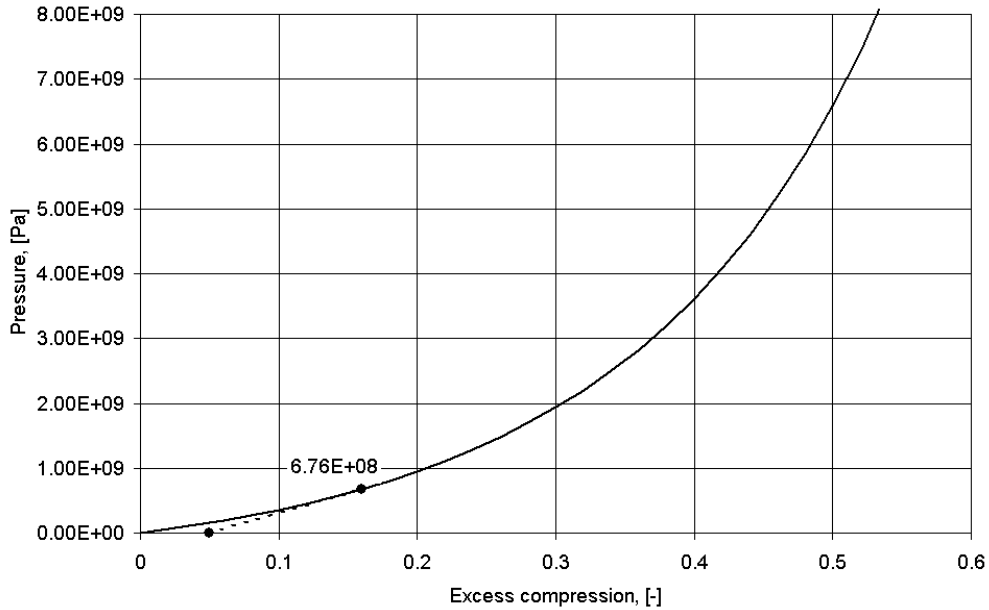


Fig. 4 The Tensor pore collapse EOS, used for saturated sandy clay. The excess compression is defined as  $\mu = \rho/\rho_0 - 1$  and the hydrostatic pressure  $p = (\sigma_1 + \sigma_2 + \sigma_3)/3$ .

#### 4.4 Concrete With Reinforcement

RC 90 is made of C30 grade concrete (Swedish code, K40), [12]. The outer walls are reinforced utilising two layers of orthogonal bars of  $\Phi 14$  [mm], cc 200 [mm]. Steel quality: yield stress 400 [MPa], (ks 400). Cover layer is 40 [mm].

The material model Concrete damage, [13]-[15] is used with the EOS, Tabulated compaction. The initial density of the concrete is 2230 [kg/m<sup>3</sup>]. The utilised material properties are shown in table 1.

Table 1. Material properties for Concrete damage model

Property	Value	Property	Value
Poisson's ratio, [-]	0.19	Press. hardening coeff., yield, $A_{2f} \cdot 10^9$ , [-]	3.101
Max principal stress for failure, [MPa]	2.9	Compressive damage scaling factor, $b_1$ , [-]	1.5
Cohesion for max., $A_{0m}$ , [MPa]	11.3	Tensile damage scaling factor, $b_2$ , [-]	2.0
Pressure hardening coeff., $A_{1m}$ , [-]	0.446	Triaxial tensile damage s. factor, $b_3$ , [-]	2.2
Press. hardening coeff., $A_{2m} \cdot 10^9$ , [-]	2.120	Percent reinforcement, [%] <sup>(1)</sup>	1.92
Cohesion for yield, $A_{0y}$ , [MPa]	8.513	Elastic modulus for reinf., [GPa] <sup>(1)</sup>	200
Press. hardening coeff., yield, $A_{1y}$ , [-]	0.625	Poisson's ratio for reinf., [-] <sup>(1)</sup>	0.3
Press. hardening coeff., yield, $A_{2y} \cdot 10^9$ , [-]	6.751	Initial yield stress for reinf., [MPa] <sup>(1)</sup>	400
Press. hardening coeff., failed, $A_{1f}$ , [-]	0.442	Plastic hard. modulus for reinf., [MPa] <sup>(1)</sup>	500

Comment (1): Used only for the smeared reinforcement elements

Because the reinforcement is treated isotropically and no failure strain can be defined, the validity of the reinforcement modelling may be subject to discussion.

The material model has three pressure hardening failure surfaces, yield, maximum, and residual failure surface:

$$\Delta\sigma_y = a_{0y} + \frac{p}{a_{1y} + a_{2y} \cdot p} \quad (\text{yield failure surface}) \quad (3)$$

$$\Delta\sigma_m = a_{0m} + \frac{p}{a_{1m} + a_{2m} \cdot p} \quad (\text{maximum failure surface}) \quad (4)$$

$$\Delta\sigma_r = 0 + \frac{p}{a_{1f} + a_{2f} \cdot p} \quad (\text{residual failure surface}) \quad (5)$$

$$\text{With the stress difference, } \Delta\sigma = \sqrt{3 \cdot J_2} \quad (6)$$

In the model linear interpolation is performed between yield and maximum surface after the yield surface is reached, equation (7). The scale factor,  $\eta$  varies between 0 and 1 [-]. It is dependent on the accumulated effective plastic strain parameter,  $\lambda$ , see figure 6. After the maximum failure surface is reached, the actual surface is interpolated in similar way between maximum and residual surface, equation (8).

$$\Delta\sigma = \eta(\Delta\sigma_m - \Delta\sigma_y) + \Delta\sigma_y \quad (7)$$

$$\Delta\sigma = \eta(\Delta\sigma_m - \Delta\sigma_r) + \Delta\sigma_r \quad (8)$$

In figure 5 and 6 the utilised failure surfaces and tabulated damage function are shown. The utilised EOS is shown in figure 7. The strain rate enhancement factor is specified as a tabulated function. The utilised data compiles to CEB-FIP Model Code 1990 recommendations for compressive strength for strain rates  $\leq 30$  [1/s], see figure 8, [12].

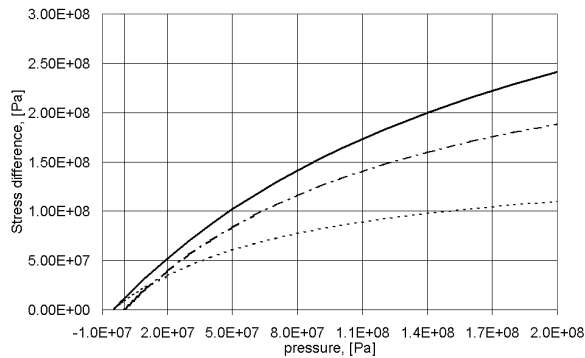


Fig. 5 Failure surfaces utilised, — : maximum, - - - - : yield, — · — · — : residual

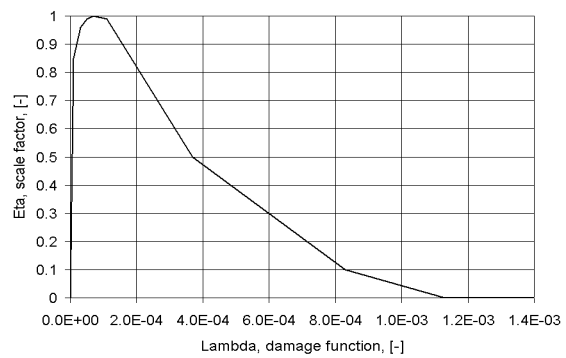


Fig. 6 Tabulated damage function,  $\lambda$  versus  $\eta$

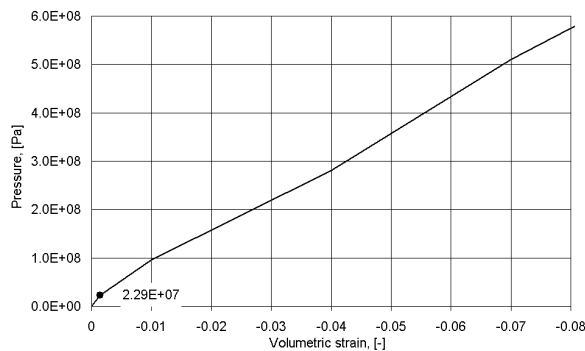


Fig. 7 EOS utilised, the unloading bulk modulus:  $K_u=15.6$ [GPa] for  $p \leq 22.9$  [MPa],  $K_u=28.1$  [GPa] for  $p > 22.9$  [MPa].

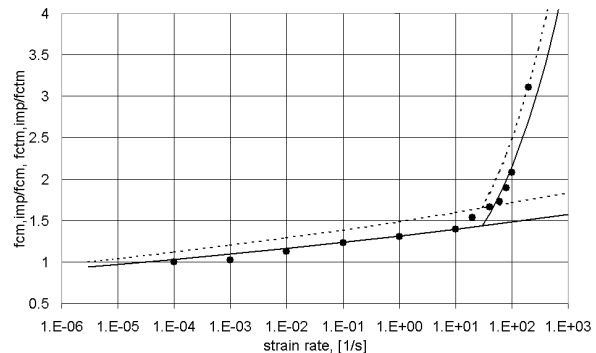


Fig. 8 Strain rate enhancement according to CEB-FIP Model, — : compressive, - - - - : tensile, [12] and single element test, ● : compressive

Uniaxial, quasi-static, single element tests are performed and compared with CEB-FIP Model Code recommendations for stress-strain curves for grade C30, see figure 9 and 10. The length of the element is 200 [mm], with a constant cross section 100-100 [mm<sup>2</sup>]. A constant loading velocity is used,  $\pm 2 \cdot 10^{-5}$  [m/s], thus the strain rate in the test is  $1 \cdot 10^{-4}$  [1/s]. The 4 nodes at bottom are locked in loading direction.

Methods to produce dynamic deformation are discussed in [16]. Single element tests with different strain rates are performed, see figure 8. The tests show that the enhancement factor for strain rates above 30 [1/s] will be taken into account in the calculation without adding the second part that CEB-FIP Model Code recommends. Constant velocities are used for the tests, thus the acceleration in loading direction is zero, the strength enhancement develops because a multiaxial stress state occurs for higher strain rates.

Strain rate effects in concrete and explicit solution methods are discussed in [17]. In [17] it has been concluded that the strength increase will result from inertia effects.

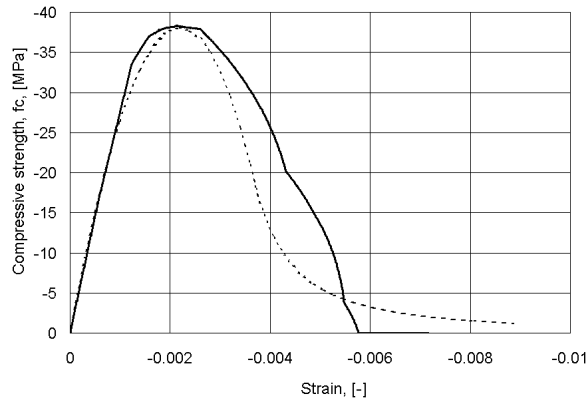


Fig. 9 Stress-strain diagram for concrete in compression. — : Single element test, - - - : CEB-FIP Model

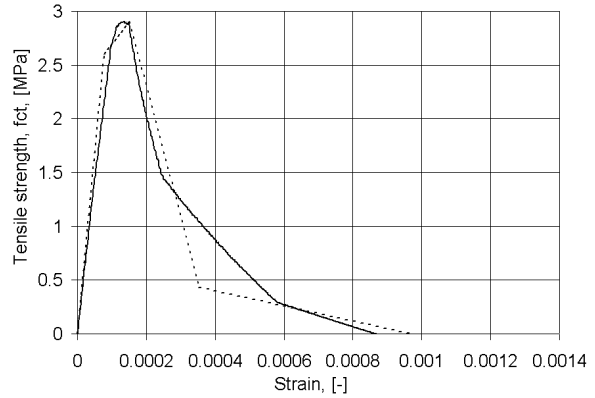


Fig. 10 Stress-strain diagram for concrete in tension. — : Single element test, - - - : CEB-FIP Model, (aver. crack distance= 200 [mm])

### 5. Partially buried weapon (50 percent) with offset distance, 5 [m] to RC 90

The main part of the loading on the RC 90 is a result of the ground shock for the type of soil and geometry considered, thus the ground shock will be further discussed. In figure 11-14 the ground pressure and velocity are shown and compared with [4].

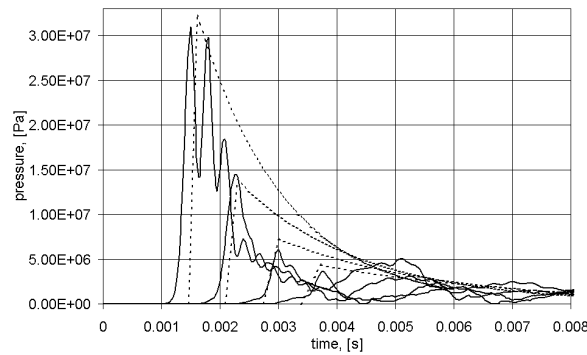


Fig. 11 Ground pressures, at depth 1.5 [m], horizontal distance, 2, 3, 4, and 5 [m] from weapon. — : FE-model, - - - : according to [4]

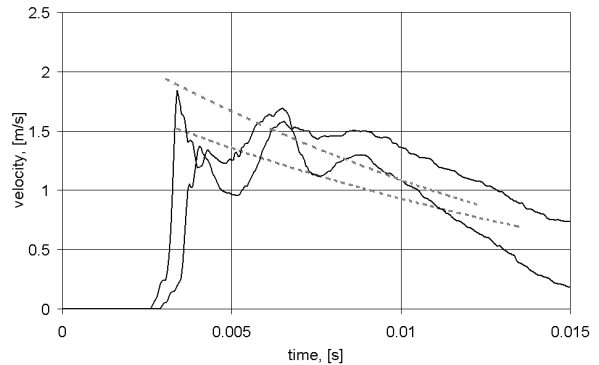


Fig. 12 Ground velocities, at depth 1.5 [m], horizontal distance, 4.5, and 5 [m] from weapon. — : FE-model, - - - : according to [4]

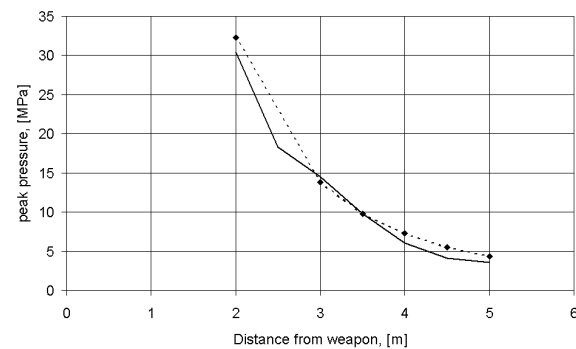


Fig. 14 Peak pressures in ground, at depth 1.5 [m] versus horizontal distance from weapon. — : FE-model, - - - : according to [4]

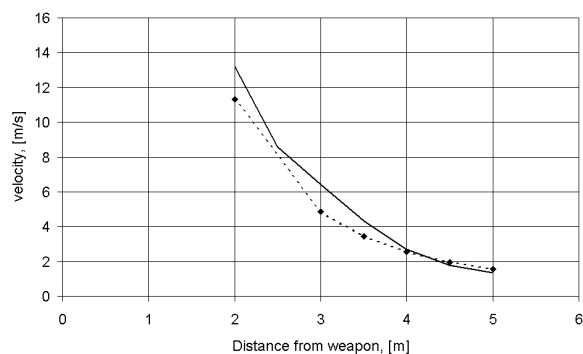


Fig. 15 Peak velocities in ground, at depth 1.5 [m] versus horizontal distance from weapon. — : FE-model, - - - : according to [4]

The response of the bottom floor of the structure is shown in figure 16. It is compared with the semi-empirical formulae presented in [18], and [19]. The inner wall is assumed to be a simply supported plate with the dimensions, 6, 2.875, and 0.5 [m] in the semi-empirical formulae.

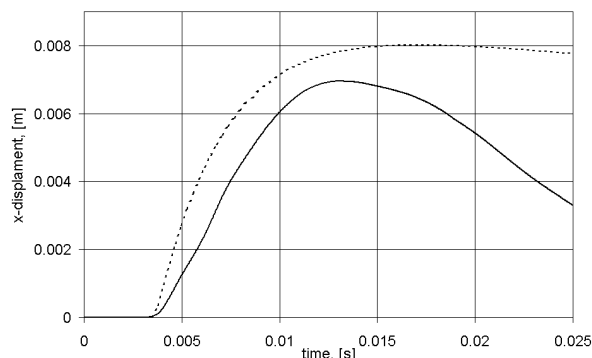


Fig. 16 The outer wall response, at depth 1.5 [m].  
 — : FE-model, - - - : according to [18].

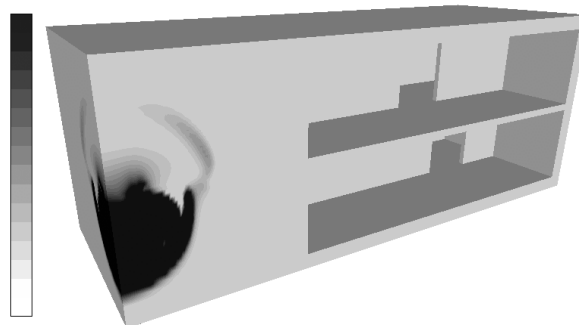


Fig. 17 Pressure plot at time 1 [ms], fringe scale 0 to 5 [MPa].

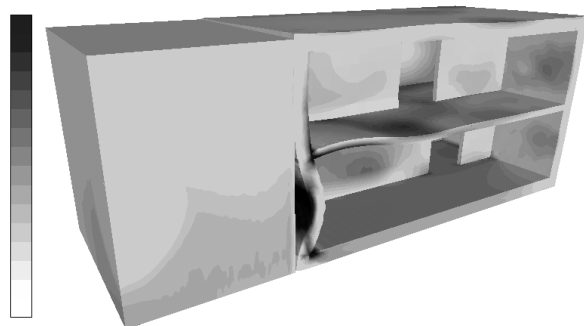


Figure 18. Pressure plot at 14 [ms], fringe scale 0 to 5 [MPa]. (scaled displacements)

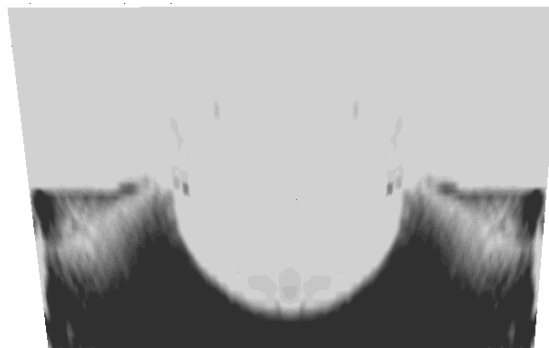


Figure 19. The crater at time 25 [ms].

In figure 17, the separation of air blast and ground shock can be seen, the maximum response in figure 18, the generated crater in the ground in figure 19, visualised with Glview 5.1 [20].

## 6. Conclusions

- Using multi-material fluids in the simulation makes it possible to account for the air blast and ground shock. The shape of the crater compares fairly well with [4].

- The computed ground shocks, peak pressures, peak velocities, and the decrease of slope of the shock front in the ground are in excellent agreement with [4].

- Accounting for fluid /structure interaction allows the structure to separate from the fluid, which gives a qualitative prediction of the structural response.

- The use of a material model that takes the deviatoric stresses into account in this type of soil is important in the unloading phase of the ground pressures.

- The crater's shape and dimensions seem to influence the unloading phase of both pressure and velocity histories, further investigations are needed in this matter.

- The single element tests on the concrete model show that uniaxial compressive and tensile paths can be predicted. It is also concluded that strain rate enhancement above 30 [1/s] occurs due to confinement.

- The modified gamma law with an added constant for the air is important for avoiding computational difficulties in multi-material fluids.

## **7. References**

- [1] "LS-DYNA USER'S MANUAL" Version 940, Livermore Software Technology Corporation, 1997
- [2] "ANSYS/LS-DYNA, Theoretical Manual, For Release 5.5", ANSYS, Inc., 1998
- [3] "LS-DYNA3D COURSE, Fluid / Structure Coupling", *Dynalis-ChE-26-06-98*, DYNALIS, 1998, 1-10
- [4] "Fundamentals of Protective Design for Conventional Weapons", TM 5-855-1, U.S. Army Engineer Waterways Experiment Station, 1992
- [5] "ANSYS/LS-DYNA, User's Guide, for release 5.5", ANSYS, Inc., 1998
- [6] "AUTODYN<sup>TM</sup>, Theory Manual, Rev. 3.0", Century Dynamics Inc., 1997
- [7] "LLNL EXPLOSIVES HANDBOOK, Properties of Chemical Explosives and Explosives Simulants", Lawrence Livermore National Laboratory, 1985
- [8] Rollvik, S., Sjøl, H., "COMPARISON OF SOME DIFFERENT FORMULAE FOR GROUND SHOCK PREDICTION", (in Norwegian) Norwegian Defence Research Establishment, FFI, 1991
- [9] Das, B., M., "Principles of Geotechnical Engineering", PWS-KENT Publ. Comp., 1990
- [10] Fredlund D., G., Rahardjo, H., "SOIL MECHANICS FOR UNSATURATED SOILS", John Wiley & Sons Inc., 1993
- [11] Karig, D., E., "Experimental and observational constraints on the mechanical behaviour in the toes of accretionary prisms", *Deformation Mechanisms, Rheology and Tectonics*, The Geological Society, No 54
- [12] CEB, "CEB-FIP Model Code 1990, Design Code", Thomas Telford, 1993
- [13] Malvar, L., J., Crawford, J., E., Wesevich, J., W., "A NEW CONCRETE MATERIAL MODEL FOR DYNA3D", Karagozian & Case, 1994
- [14] Malvar, L., J., Crawford, J., E., Wesevich, J., W., "A NEW CONCRETE MATERIAL MODEL FOR DYNA3D, RELEASE II: SHEAR DILATION AND DIRECTIONAL RATE ENHANCEMENTS", Karagozian & Case, 1996
- [15] Malvar, L., J., Crawford, J., E., Wesevich, J., W., Simons, D., "A PLASTICITY CONCRETE MATERIAL MODEL FOR DYNA3D", *International Journal of IMPACT ENGINEERING*, Elsevier Science Ltd, volume 19, 1997, 847-873
- [16] Mayers, M., A., "Dynamic Behaviour of Materials", John Wiley & Sons, Inc., 1994
- [17] Johansson, M., "BETONGENS TÖJNINGSHASTIGHETSBEROENDE OCH EXPLICIT LÖSNINGSMETODIK", (partly translated into English), Chalmers University of Technology, Sweden, 1998
- [18] Balazs, P., "Methods for calculations of blast loaded structural behaviour", (In Swedish) Swedish Defence Research Establishment, FOA, 1997
- [19] Balazs, P., "Full scale test with steel reinforced concrete slabs in sand subjected to ground shock from detonated bombs", (In Swedish) Swedish Defence Research Establishment, FOA, 1998
- [20] "Glvie 5.1", ViewTech AS, Norway, 1999